JOURNAL OF MATERIALS SCIENCE 25 (1990) 2287–2298

Dynamic consolidation of cylinders by oblique shock loading

K. P. STAUDHAMMER
Los Alamos National Laboratory, Los Alamos, New Mexico 87545
L. E. MURR
Department of Metallurgical and Materials Engineering, The University of Texas at El Paso, El Paso, Texas 79968-0520, USA

An oblique shock loading arrangement is utilized to dynamically consolidate small diameter solid and hollow cylinders of type 304 stainless steel and tungsten. The experimental arrangement approximates a 2-dimensional consolidation regime when viewed along any plane perpendicular to the cylinder axes. Hot spots and localized melting were observed to occur in regions characterized by interstitial or other void space prior to consolidation due to extrusion of matter into these spaces creating strain heating. The larger the void spaces, the more preponderous the melting. In consolidating hollow cylinders where the internal void area was larger than the interstitial void area, the melt preponderance shifted to the tube centers. By filling void space using solid cylinders of various diameter to approximately a 2-dimensional "particle" size distribution, void space could be minimized and local heating and melting reduced or eliminated. The melt fraction was also observed to increase with increasing peak shock pressure in the range of 12 to 22 GPa.

1. Introduction

In a recent summary of the current understanding and theories (or models) relating to the actual dynamic consolidation of particulate materials (at high strain rates), Linse [1] concluded that densification and interparticle bonding mechanisms that occur on a particulate scale during dynamic/explosive compaction processes are extremely complex. The transition from an unconsolidated state (prior to shock compaction and consolidation of powders) to a fully dense state, or a regime characteristic of a contiguous solid, necessitates that the particles deform, flow to fill void space, and form interparticle bonds. This process, accordingly, is facilitated by deformation heat which softens particles, thereby increasing ductility. Taniguchi *et al.* [2] have also concluded that plastic flow of particles is essential in the dynamic compaction process of ductile metal particles. While plastic flow is essential, however, it is a result of the compaction process, not a requirement, and without it there would not be consolidation. The consolidation event is far more complicated than that alluded to above. Only the portions of the particle undergoing deformation or localized extrusion to fill the voids realize the high localized temperatures. A portion of each particle (the amount being a function of the particle size) is not softened but may undergo considerable shock hardening.

Wilkins *et al.* [3], in summarizing dynamic powder consolidation from a more theoretical perspective, have also concluded that many materials exhibit considerable ductility in the high-pressure state, and that substantial plastic flow occurs from the high pressures of dynamic loading. They conclude that consolidation of powders results from the local welding of adjacent particles. But earlier work by Morris [4] concluded that bonding mechanisms for powder consolidation appear to be essentially the same as those operating during explosive bonding of (sheet or plate) metals where the role of actual melting is often completely absent.

Recent models, both phenomenological and theoretical, have dealt with shock-wave consolidation of powders (particularly metal powders) in the context of the fraction of (or prominence of) energy deposition near particle surfaces as opposed to energy dissipation in plastic deformation in particle interiors, etc., and the role of pressure, shock duration, and particle size on the integrity of the final, consolidated product, the melt fraction within the product, crack production, and the optimization of these interrelated parameters [5–11]. Based upon these more recent and popular models, it is concluded that melting or melt fraction associated with powder consolidation depends upon pressure and its time of application, as well as the mean particle size. Assuming monosize spherical particles, surface temperature (or energy deposition at particle surfaces), increases with increasing particle diameter. In addition, such energy deposition has been assumed to be uniform over the particle surface or in a near-surface region [6, 8]. Therefore, increasing the packing density (and a corresponding decrease in void volume) reduces melting. Nearly all models to date, although dealing with different particle sizes, have dealt with monosize spherical particles. While

0022–2461/90 $03.00 + .12

Gourdin [7] has alluded to the prospects that a broad size distribution of particles will decrease the average surface temperatures, models to date have not treated even bimodal distributions, and none have explicitly treated irregular or even nonspherical particles, although in the implosive consolidation of plate-like, irregular amorphous particles, Murr *et al.* [12, 13] have observed no evidence of interparticle melting. Very early work by Cline and Hopper [14] on amorphous powders also demonstrated that shock-wave consolidation occurs without any apparent crystallization or structural modification.

It is particularly intriguing to consider that current HIP models for elevated temperature densification of powders have also considered only monosize particles, and assume uniform deformation of individual particles. In practice, however, powders subjected to HIP usually have a distribution of sizes. Nair and Tien [15] have recently found that in developing a model for HIP based upon a bimodal distribution of spherical particle sizes, the smaller particles bear the burden of higher interparticle stresses and plastic strains. They assert that for the case of a full size distribution of particles, all would generally deform to different extents.

Lotrich *et al.* [16] have also recently proposed a thermal deposition model to describe the inhomogeneous temperature distribution seen to occur in many dynamically compacted powder regimes in which air, at some temperature and pressure in the voids, or interparticle interstices, plays a significant role. In this model, thermal deposition occurs between or among impacting particles by the shock compression of the gas (air) in the voids upon pore collapse, with subsequent deposition of the heat generated in the gas at the particle surfaces. The idea that adiabatic heating of gas or a gas-phase regime within the solid particles is a source for interparticle melting is indeed an intriguing approach because it focuses on void space as a principal feature of the shock compaction/consolidation process.

Williamson *et al.* [17] have previously described the localized transport or displacement of spherical particle surface material from the areas of contact into the interstices or void spaces during consolidation. Both experimental observations and recent modelling of idealized (spherical) alloy RSP powders have shown that when the material is densified, some parts of the spheres deform and fill the void spaces by the extrusion of matter while other parts of the spheres deform to change a point of contact with neighbouring spheres until the expanding contact circles meet [18, 19]. Greater strain is encountered in the areas where deformation occurs to fill the void spaces. Heat is generated from local plastic deformation and if the strain rate is high (as it is in shock wave consolidation), this localized heating within a spherical particle regime cannot be dissipated by conduction. Consequently, high-temperature spikes occur in the high strain areas characterized by void spaces which can exceed the melting point [17 – 19]. These so-called hot spots are observed experimentally and can be

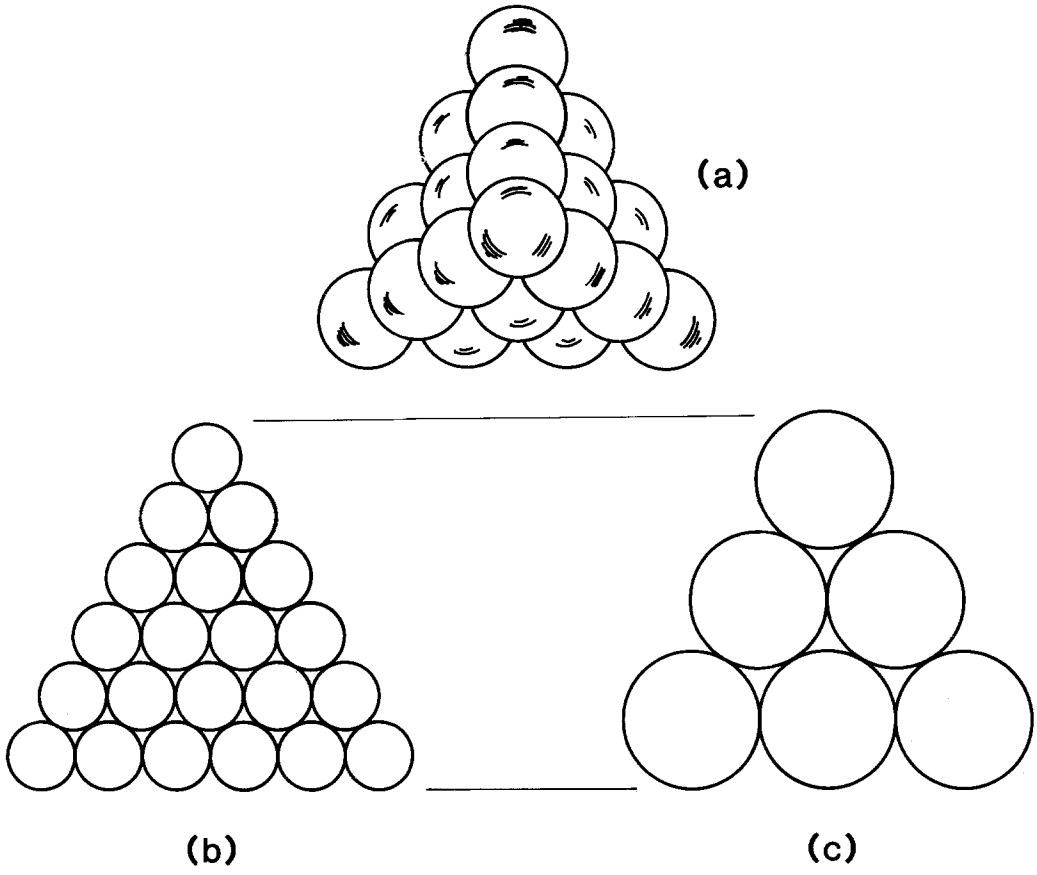

Figure 1 Ideal packing of monosize (spherical) particles in 3-dimensions (a), and schematically represented two-dimensionally (b, c). As the diameter increases [(b to c)], the interstices or void spaces between spheres increases correspondingly. Total void space is also increased, but at a smaller rate.

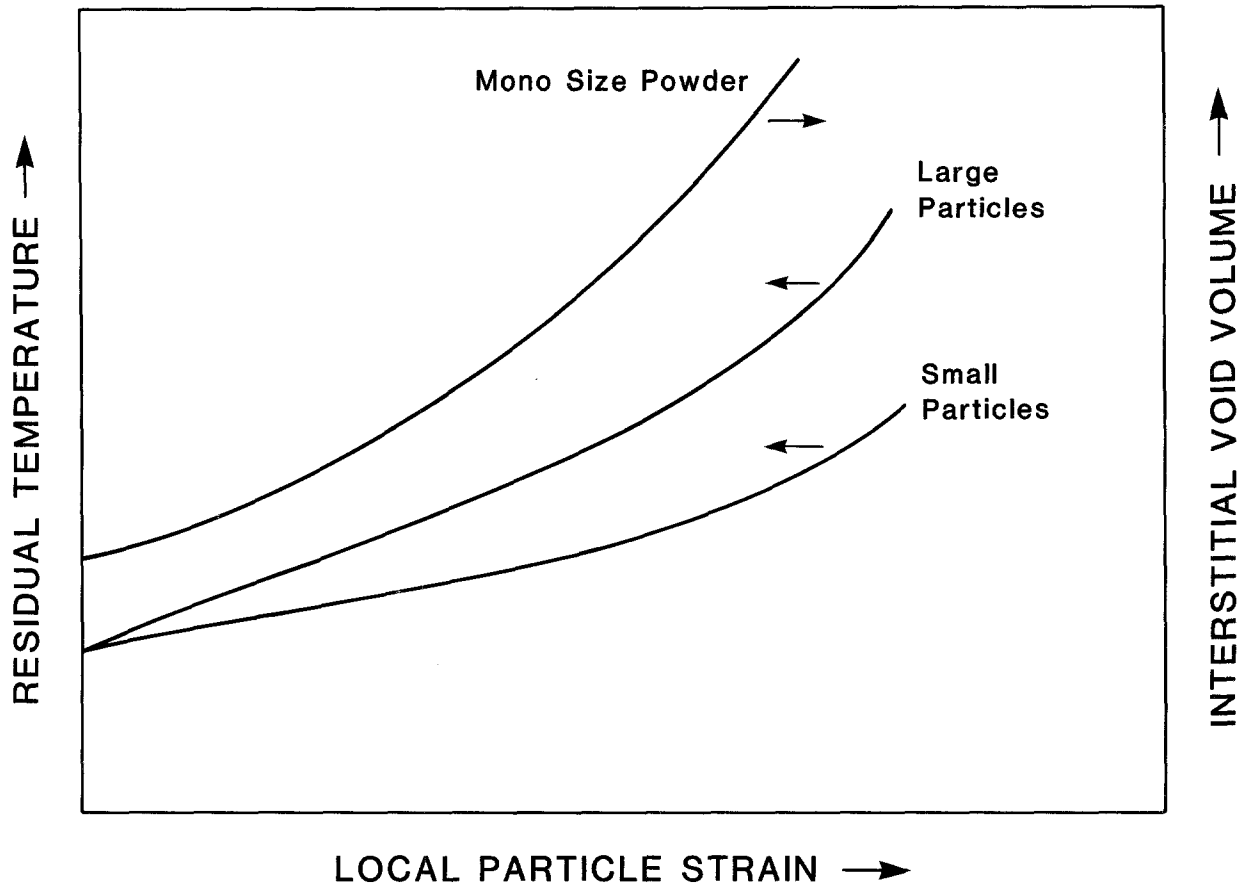

Figure 2 Representation of the change in residual temperature with local particle strain for small (spherical) particles and large particles as depicted in Fig. 1(b and c), respectively, and the variation of local particle strain with interstitial void volume.

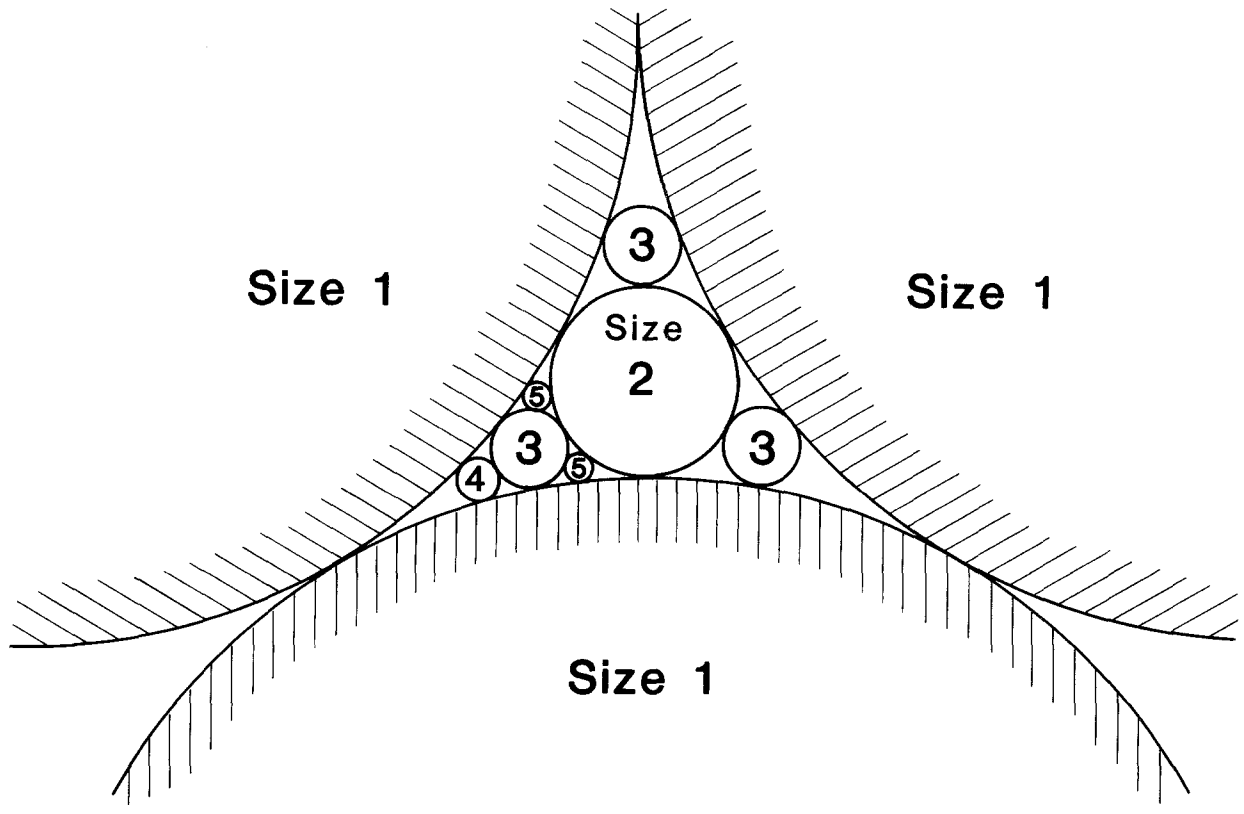

Figure 3 Two-dimensional view of interstitial void filling by including a range of smaller, distributed particles amongst a large (or coarse) monosize particle regime (size 1).

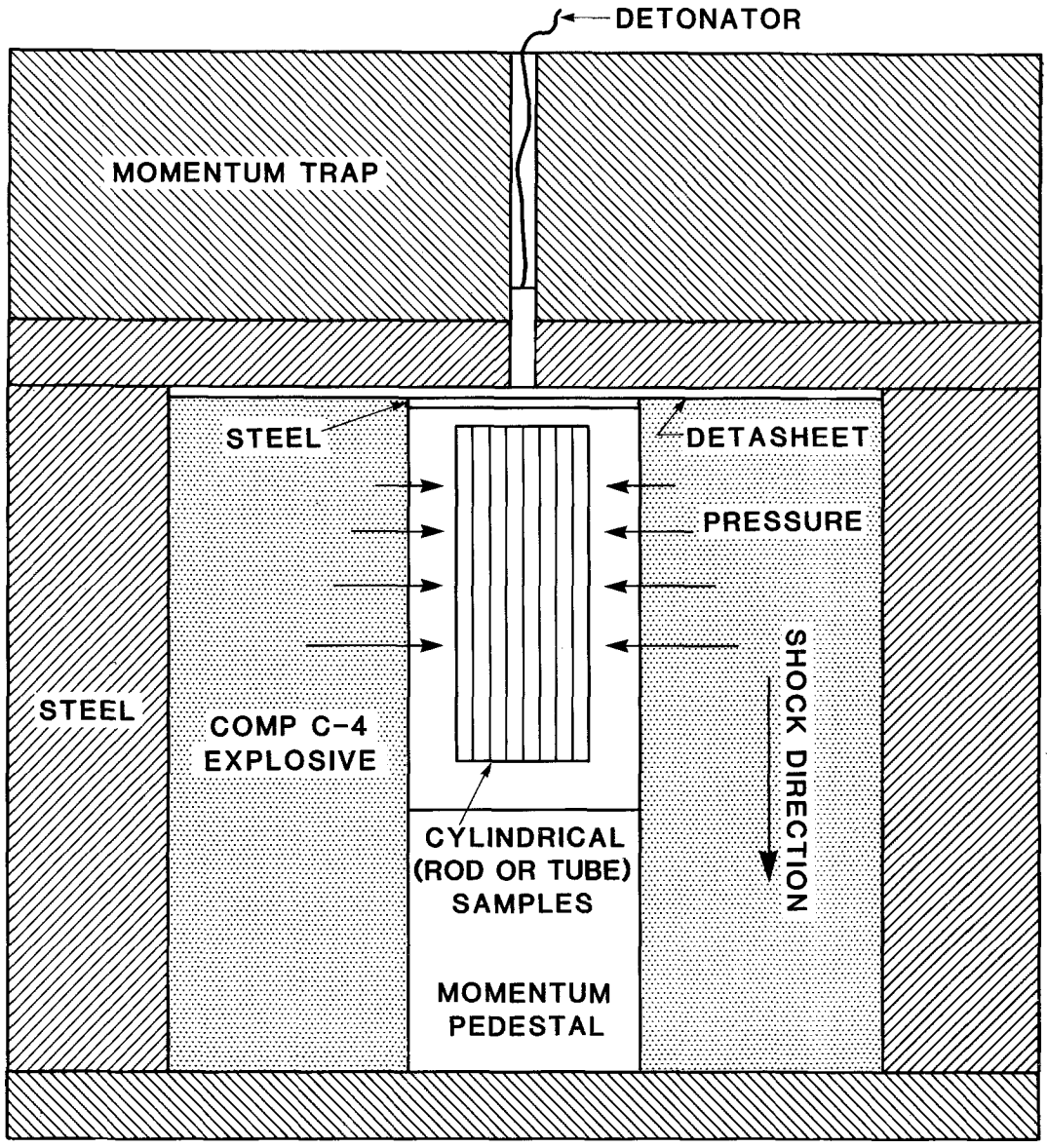

Figure 4 Implosive (shock compression) loading assembly for consolidation of cylindrically symmetric metal rods or tubes. In the arrangement shown, the shock pressure is applied around the circumference of the tube specimen arrangement and traverses down the sample axis, which is into the page in Fig. 5 following along the shock direction shown.

reasonably well modelled using 2-dimensional numerical calculations [17–19].

If we examine the recurring elements in the dynamic compaction and consolidation experiments and models briefly reviewed above [1–19], it is apparent that strain associated with void space filling seems to be a controlling feature of heating and melting during dynamic consolidation and, thereby, a controlling feature of the process itself. On the other hand, the experiments have been mostly concerned with idealized, spherical, monosize, 3-dimensional particle regimes while the models, and the process representations, have been 2-dimensional. And like the HIP process (15), dynamic consolidation is often (practically) accomplished in bimodal or multi-modal powder size distributions which are not represented by the experiments with monosize spheres or 2-dimensional models of such regimes.

In the present investigations, we sought to develop an experimental regime more representative of a 2-dimensional, dynamic consolidation process which could be analyzed and modelled in a 2-dimensional format as well. To accomplish this, we have devised a series of experiments involving the oblique explosive (implosive) shock-wave consolidation of small diameter metal cylinders.

2. Analytical and experimental details

Figure 1 illustrates somewhat phenomenologically the prominent features of this study as well as the dilemma discussed above in regard to the 2-dimensional modelling of a 3-dimensional regime. Figure 1a illustrates the ideal packing of monosize spheres prior to consolidation (which includes compaction and bonding or "welding"), while Figs 1b and c illustrate a simple 2-dimensional view or a single plane through an ideal sphere packing regime having sphere sizes greater and less than Fig. 1a. For spherical particles illustrated in Figs 1b and c, the packing (compaction) density is 74% and the corresponding void fraction is, therefore, 26%. In the context of the 3-dimensional regime, the void fraction becomes the void volume or porosity.

If we treat the void volume or porosity phenomenologically in terms of the geometries presented in

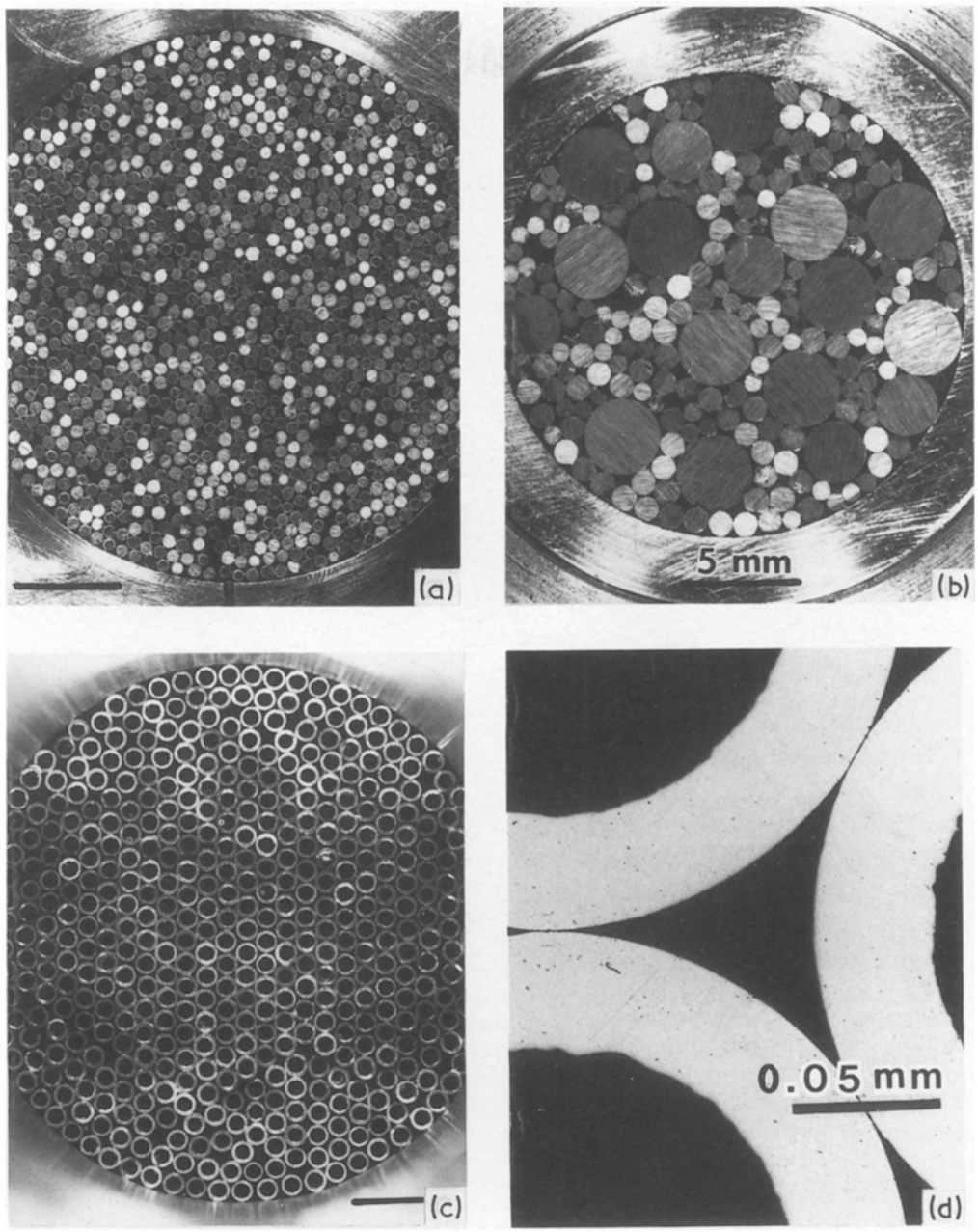

Figure 5 Typical distribution of solid, monosize rods (tungsten) in (a) and a trimodal distribution of tungsten rods (3 separate rod diameters) showing void distribution (b). The views in (a) and (b) are at 90° to the consolidation schematic shown in Fig. 4. In (a), (b) and (c), the shock direction shown in Fig. 4 is into (normal to) the page. (c) A sample assembly of 304 stainless steel monosize tubes prior to explosive (implosive) consolidation. (d) Enlarged view of area in (c) showing the preponderance of tube void space against interstitial (interparticle) void space implicit in Fig. 3.

Figs 1b and c, we can observe that full density in consolidation will require the elimination of the porosity by collapse of the voids. It is obvious that if we treat the void filling in terms of particle deformation to fill the space as depicted in Figs 1b and c, there are more discrete deformation sites in Fig. 1b while the deformation (or straining) to fill void sites is much greater in Fig. 1c. If the temperature rise during compaction and consolidation, and the residual temperature after consolidation, is primarily an accumulation of localized heating within spherical particle regimes as a result of local straining to fill void space, then as the void volume increases, the local particle strain would be expected to increase correspondingly, and increase the residual temperature. With Fig. 1b representing a fine-particle regime and Fig. 1c representing a course particle regime, the corresponding temperature variations during or after consolidation might be depicted phenomenologically as shown in Fig. 2. Figures 1 and 2, in particular Figs 1b and c and Fig. 2 could also be considered to represent a region with a volume of particles or a distribution of particles. In other words, by varying the particle size, the void size will change correspondingly, and this can be used as a means of systematically altering overall temperature or local temperature in a dynamically consolidated sample. Since void size and distribution are important in localizing strain and temperature during consolidation, filling the void or interstitial spaces with smaller particles, as shown in Fig. 3, will distribute and reduce the strain temperature.

To test the features implicit in Figs 1 to 3, we

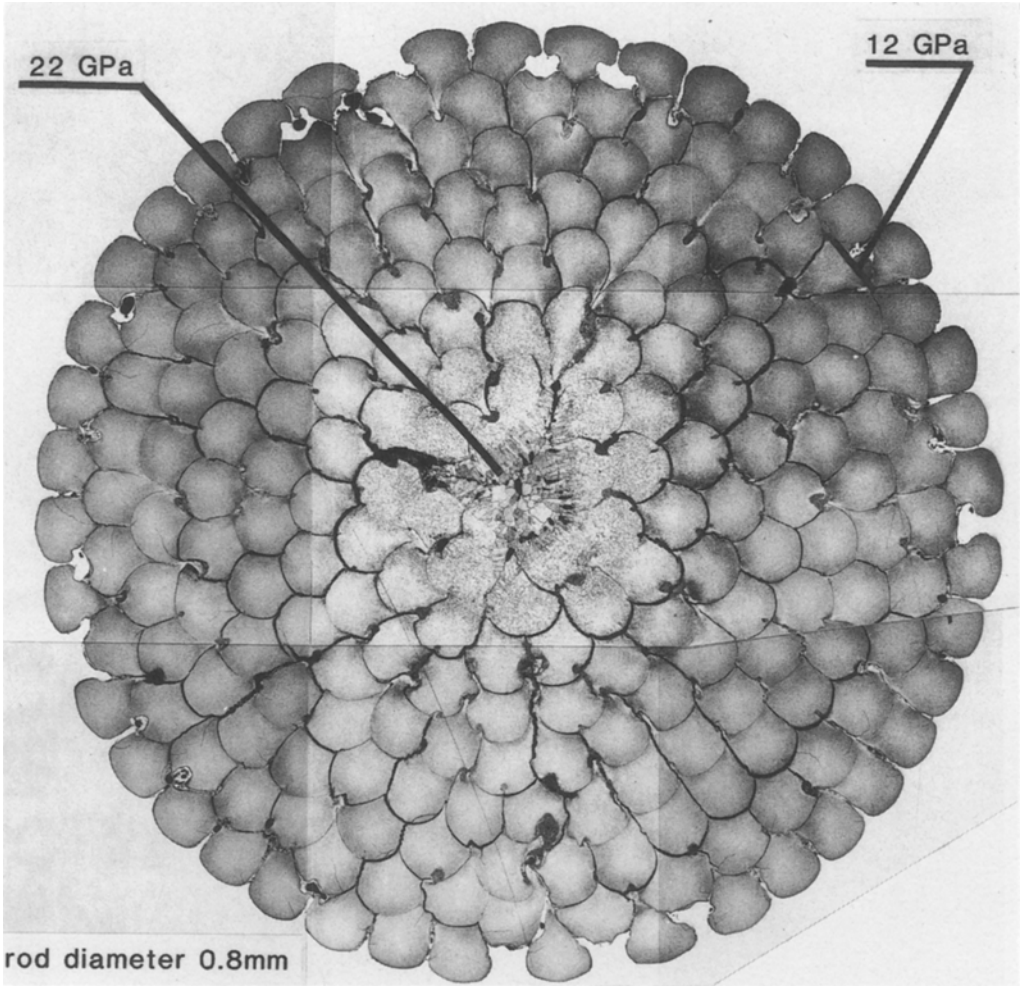

Figure 6 Metallographic (cross-section) view of implosively consolidated 0.8 mm diameter (monosize) tungten rods. Pressure difference across the specimen plane is indicated. (22 GPa in the centre to 12 GPa around the circumference of the consolidated regime.)

designed a series of experiments based upon the cylindrical shock loading arrangement shown in Fig. 4. In this arrangement, cylinders or rods of either 304 stainless steel and tungsten were implosively consolidated by the cylindrical, oblique shock wave to produce an approximate 2-dimensional loading arrangement ideally depicted in Figs 1b and c.

We chose to compare the shock consolidation of 304 stainless steel rods with tungsten rods because these two materials represent a board range of melting points (1450° C and 3425° C, respectively), which could be compared in the context of the temperature implications of Fig. 2. Separate consolidation events were conducted using different monosize rods (solid cylinders) of 304 stainless steel (0.6 mm, 1.1 mm, and 1.6 mm diameter) as well as tungsten (0.8 mm, 1.6 mm, and 3.2 mm diameter). In addition, a trimodal distribution of 304 stainless steel rods was consolidated to simulate a 2-dimensional regime having these distributed sizes. Finally, tubes of 304 stainless steel having diameters consistent with some of the solid rods were implosively consolidated. This included monosize tubes consolidated in separate shock (implosive) events as well as trimodal distributions of tubes (3 different tube sizes intermixed in the same experimental cylinder). Figure 5 illustrates some of the specific experimental regimes including solid cylinders (solid tubes or rods) of type 304 stainless steel described above.

It is particularly notable to consider the tube experiments illustrated in Figs 5c and d. As shown in Fig. 5, the void fraction in the case of the tubes in Fig. 5c is enormous in comparison to that in the case of solid rods in Fig. 5a. In addition, as shown in Fig. 5d, the tube centres now represent the largest void fraction rather than the interstices between the packed tubes. Consequently, localized melting which might be expected to occur (at sufficiently large pressures) in the interstices of large stainless steel rods would be expected to move to the stainless steel tube centers since the strain would be much greater there. In effect, we designed these experiments to demonstrate the ability to systematically shift hot spots and melt zones within a dynamically consolidated regime, and correspondingly to control interparticle melting or melt fraction.

Consolidation experiments performed on cylinders packed in specimen tubes (Fig. 5) and imploded in the assembly shown schematically in Fig. 4 were done in a vacuum of $< 10^{-3}$ torr. This was accomplished by evacuating the specimen tubes which were sealed at both ends with end plates; one containing a small vacuum port which could be sealed off and lapped flat to allow the specimen canister to be placed in the shock loading assembly (Fig. 4). Consolidation was also confirmed by mechanically testing the shock loaded canisters (in tension and compression perpen-

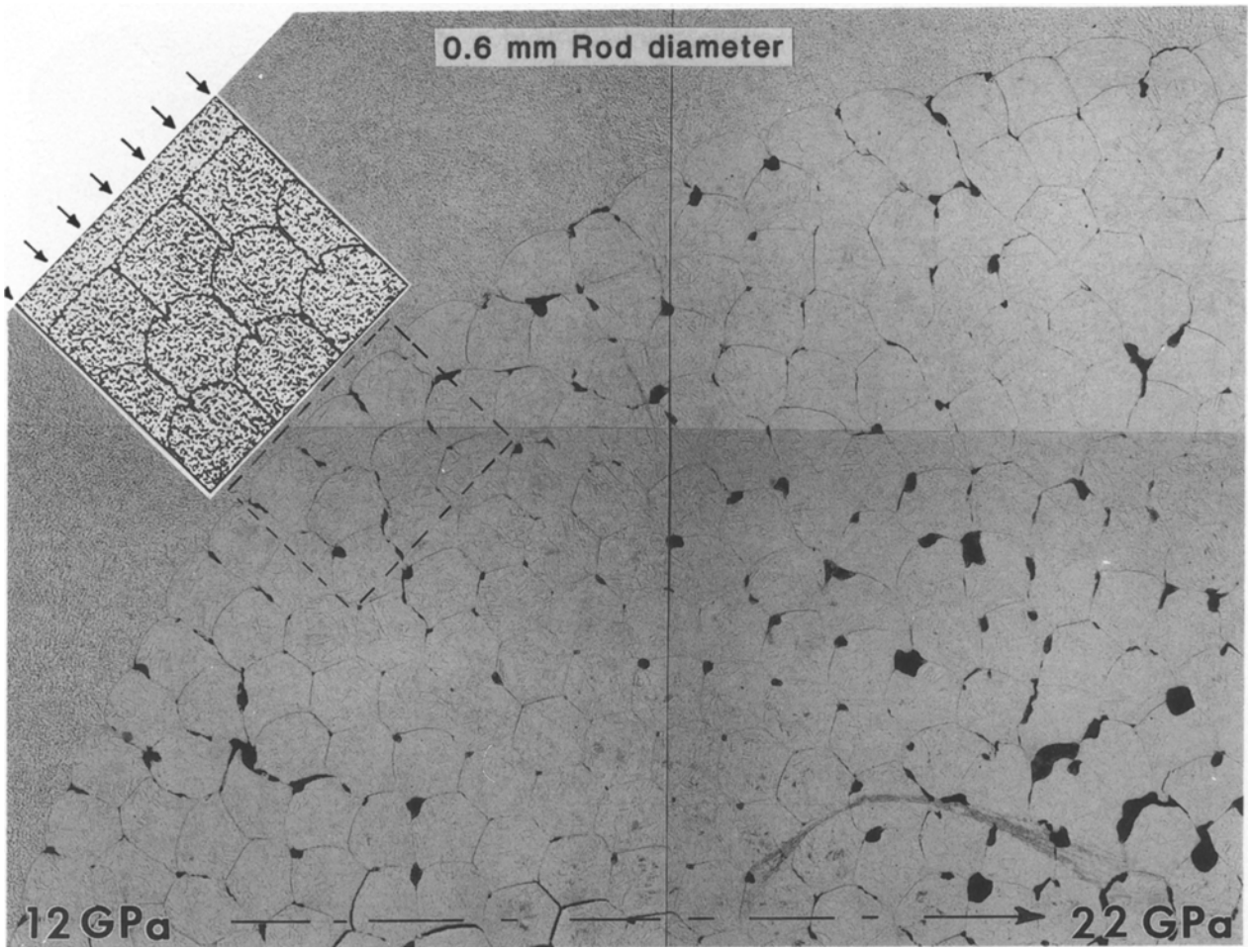

Figure 7 Metallographic (cross-section) view of implosively consolidated, monosize (0.6 mm diameter) 304 stainless steel rods. A computed view of a region shown within the dotted area is shown in the insert. The computed view is after Flinn *et al.* (19), courtesy of R. L. Williamson, INEL.

dicular to the cylinder axes) to demonstrate that the cylinders were actually bonded or "welded" together.

Computational modelling and model/experiment comparisons were also made on selected cylindrical geometries using the modelling concepts previously described by Williamson *et al.* [19]. This permitted a 2-dimensional model to be compared for the first time with 2-dimensional experiments. In addition, since the cylindrical experiments outlined above represented a range of rather coarse "particles", some comparisons were also made with fine, RSP 304 stainless steel powders consolidated in previous experiments [17–19]. This allowed us to examine and evaluate the applicability of 2-dimensional modelling to a 3-dimensional powder (particle) regime.

3. Results and discussion

Figure 6 illustrates somewhat typically the appearance of a shock consolidated series of tungsten rods (solid cylinders) which have been cut and polished to reveal the approximately 2-dimensional consolidation plane. In the implosive arrangement shown in Fig. 5, the shock pressure, characterized by an oblique, cylindrically symmetric wave indicated in Fig. 6, varies along the length of the cylindrical specimen assembly as well as within the cross-section as indicated in Fig. 6 [11]. This feature allowed comparisons of pressure effects on melt phenomena to be made within each section and at various sections along the length of the cylindrical specimen arrangement. The central or mach stem region shown in Fig. 6 illustrates the region of maximum pressure where wave convergence occurs, and where thermal effects are optimum.

Figure 7 shows for comparison with Fig. 6 the 304 stainless steel consolidation corresponding to the same pressure regime and nearly the same solid cylinder diameter as the tungsten rods in Fig. 6. Figure 7 also shows a computer model view [17] of a segment of this section which shows a nearly exact match in consolidated shape and localized melting at the locations of the initial void spaces (interstices). The irregularity in the melt zones, or the irregular sizes of the melt zones shown in Fig. 7, are a result of packing irregularities in the original assemblage which creates larger and more irregular void spaces, as evident in the unconsolidated regime illustrated in Fig. 5.

Figure 8 shows a sequence of views of shock consolidated, solid cylinders of tungsten from the same section area in separate experiments having different (monosize) diameters noted. The section areas correspond to a peak shock pressure of approximately 22 G Pa. This pressure and other pressures determined in these experiments were approximated using a LANL 2-D Eulerian hydrocode which modelled the experimental arrangement shown schematically in Fig. 4. The pulse duration or times of pressure appli-

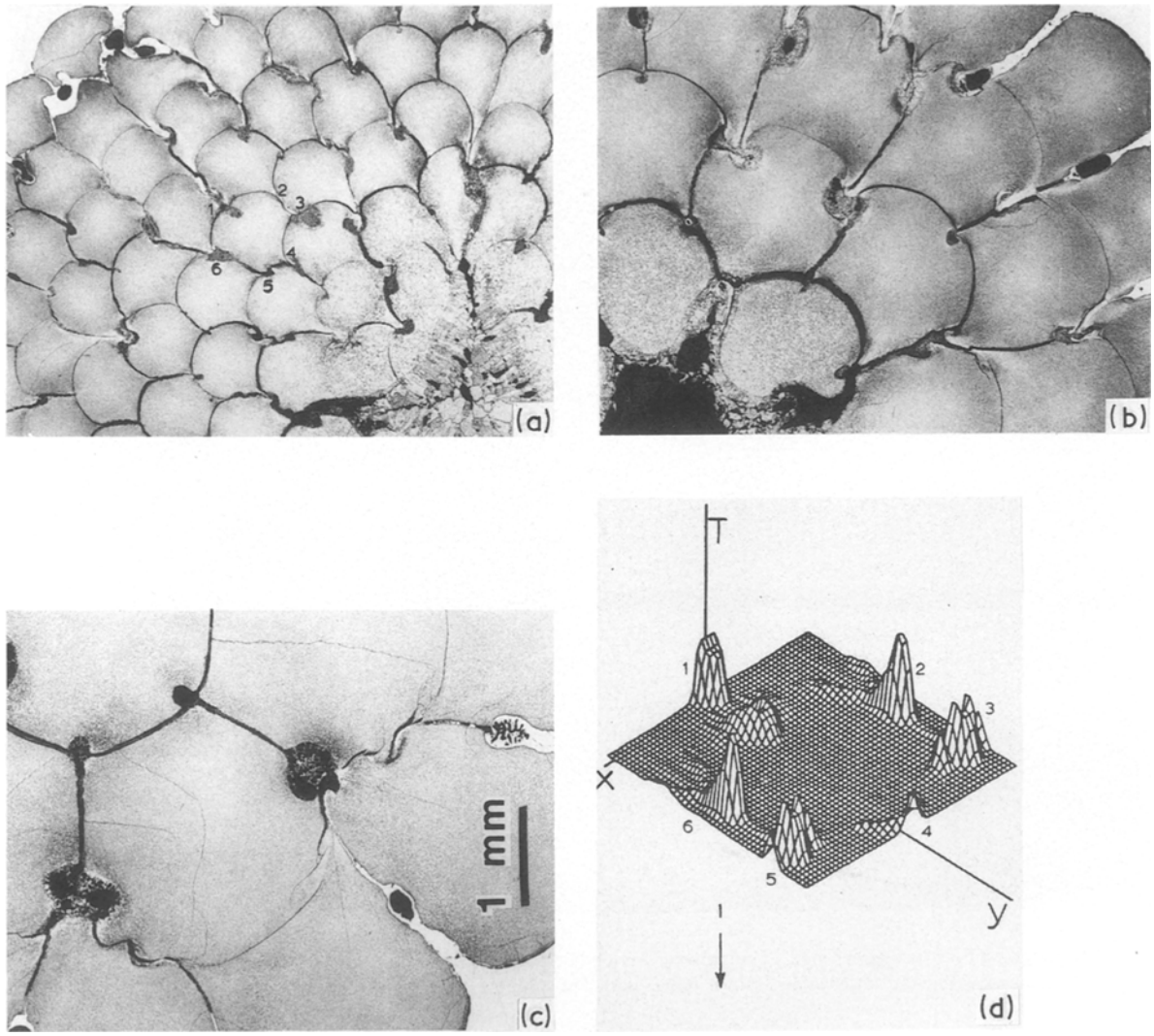

Figure 8 Metallographic section views for a series of implosively consolidated monosize tungsten rods and comparison with 2-dimensional computational modelling results for individual particles. (a) 0.8 mm diameter rods, (b) 1.6 mm diameter rods, (c) 3.2 mm diameter rods, (d) shows a computed view of the temperature profile for an individual, 2-dimensional particle as indicated in (a). (After Ref. 19, courtesy of R. L. Williamson, INEL.)

cation were also observed to be roughly 1 μs. The computed temperature profiles from the 2-dimensional model of Flinn *et al.* [19] corresponding to a time just after consolidation show hot spots which often undergo melting.

Figure 9 shows, in comparison with Fig. 8, a similar consolidation series for various solid, monosize 304 stainless steel cylinders corresponding to the same peak shock pressure ($\cong$ 22 G Pa) characteristic of the section views in Fig. 8. The computed particle temperature profile in Fig. 8a is also consistent with those shown in Fig. 9. In the actual consolidated section views in Figs 8 and 9, the melt zone size corresponding to localized heating increases with increasing cylinder diameter or 2-dimensional "particle" size. In addition, these results are consistent with the simple 2-dimensional model views shown in Figs 1b and c, and the assumption that localized straining to fill void space is the basis for localized heating. Consequently, for perfectly packed spherical "particles" or cylinders, the contacting areas will bond by local deformation, and melting will be confined to the interstices. Consequently, this view of consolidation does not require uniform surface melting around each particle, but rather localized melting governed by the size and location of the void spaces. Only the portion of the "particles" undergoing deformation or localized extrusion to fill the voids on interstitial regions represent high localized temperatures. A considerable portion of each "particle" is not softened but undergoes shock hardening. This is consistent with the recent modelling of Flinn *et al.* [19] involving 2-dimensional, numerical simulation which showed that interstitial void regions are filled by particle extrusion and represent hot spots that are often observed to have undergone melting.

This feature is further illustrated in the experiments on monosize (single diameter) tubes shown in the sequence of consolidation views in Fig. 10 corresponding to a peak shock pressure of 22 GPa. As expected on the basis of the localized strain-heating phenomena, the largest melt fractions occur within or near the tube centers and increase with increasing void fraction. Fig. 10 is also a clear indication of the ability to manipulate the melt fraction or the melt localization in dynamic consolidation, and wholly consistent with the concept of strain localization to fill void space, which we have discussed previously.

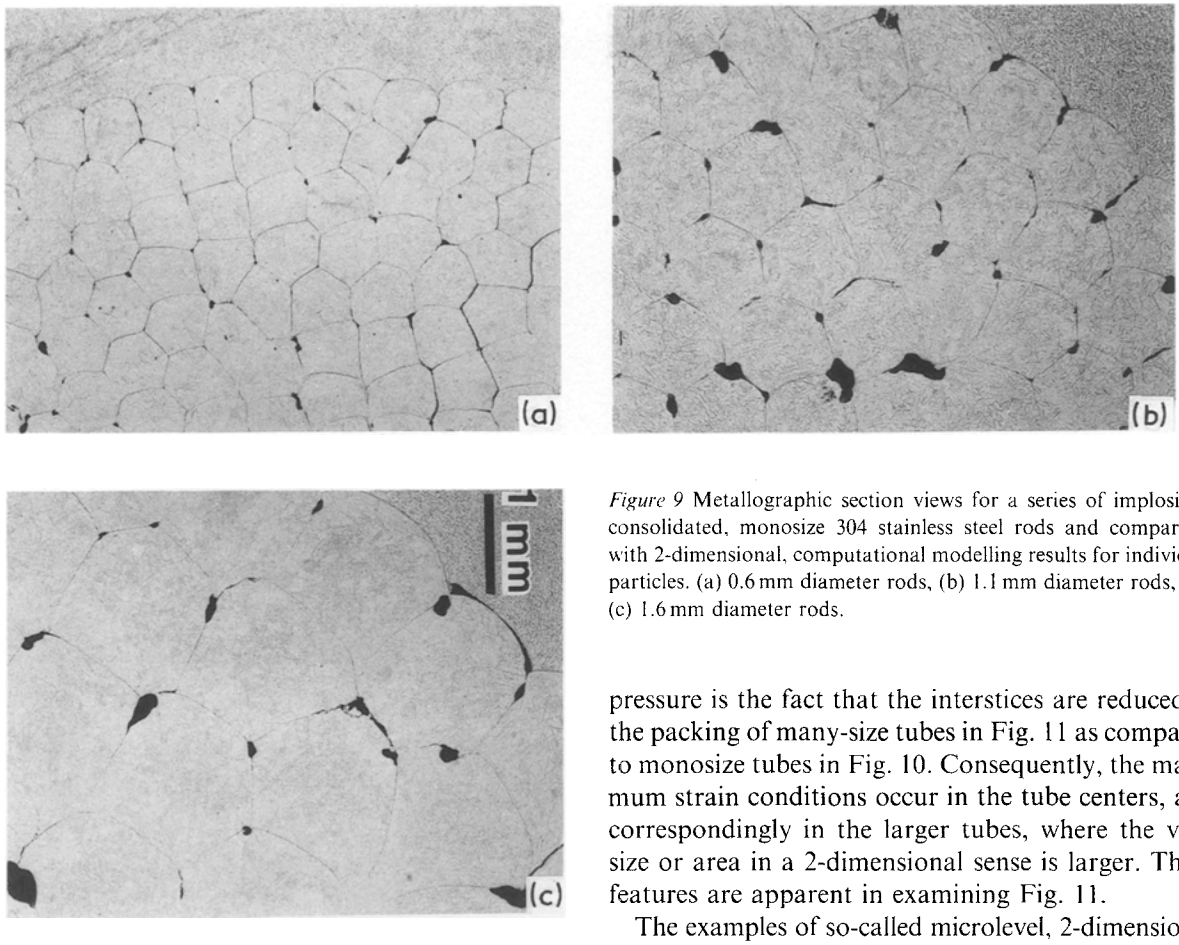

Figure 9 Metallographic section views for a series of implosively consolidated, monosize 304 stainless steel rods and comparison with 2-dimensional, computational modelling results for individual particles. (a) 0.6 mm diameter rods, (b) 1.1 mm diameter rods, and (c) 1.6 mm diameter rods.

In examining the melt localization and melt fraction in different size regimes as illustrated in Figs 8 and 9 for solid cylinders (2-dimensional monosize solids), and each size regime over a range of peak pressures, it was observed that the melt size and the melt fraction increased with "particle" size or cylinder size as well as pressure. These observations are generally consistent with previous observations for solid particles (3-dimensional solids) [1, 6, 8, 16]. However, the melt fractions are considerably less than those calculated based on uniform particle melting [6], and this has also been demonstrated in recent observations by Meyers and Wang [20].

Figure 11 illustrates the effect of size distribution and pressure on consolidation of many-size 304 stainless steel tubes (a trimodal distribution). These results are consistent with those observed for monosize solid cylinders of 304 stainless steel as well as monosize tubes (Fig. 10) in that the localized heating increases with peak shock pressure, and with the void volume, or cylinder ("particle") size. In addition, the observations in Fig. 11 also illustrate the ability to manipulate the localized melting as well as the degree of melting by controlling the void volume, void distribution, and peak pressure. In comparision with Fig. 10, Fig. 11 also illustrates the effect of utilizing a distribution of sizes to fill void space and eliminate strain localization implicit in Fig. 3. This is apparent, for example, upon examining the melting in Fig. 11 which increases with tube size and pressure; corresponding to maximum void volume as well as the strain localization. For example, the difference in melt localization in Fig. 11 as compared to Fig. 10 at the same pressure is the fact that the interstices are reduced in the packing of many-size tubes in Fig. 11 as compared to monosize tubes in Fig. 10. Consequently, the maximum strain conditions occur in the tube centers, and correspondingly in the larger tubes, where the void size or area in a 2-dimensional sense is larger. These features are apparent in examining Fig. 11.

The examples of so-called microlevel, 2-dimensional modelling included in Figs 7 and 8 (Fig. 8d) [17–19] suggests very accurate correspondence with the approximately 2-dimensional consolidation observed for solid 304 stainless steel and tungsten cylinders (solid rods) (Figs 6 to 9). Since the microlevel model has already been compared with 3-dimensional powder consolidation for micron-sized type 304 stainless steel powders, the present results lend further support not only to such modelling, but to its extrapolation or extension to 3 dimensions. The present results for shock-wave consolidated cylinders shows that melting does not occur uniformly around the perimeter of consolidated or consolidating cylinders, and this has been deduced for spherical (or 3-dimensional) particles as well [19]. It is, therefore, clear that while melting can occur around the particle perimeter (as shown for example in some areas of Figs 8 and 9), the temperature is not uniform as predicted in models of Gourdin [8] and Schwarz *et al.* [6]. Furthermore, the heating which does occur is dominated by deformation or strain (which is localized near void spaces or volume) and not by uniform shock energy deposition as proposed by Schwarz *et al.* [6] and Gourdin [8]. The present results approximating 2-dimensional consolidation are quite accurately modelled by 2-dimensional numerical analysis, which predicts hot spots at interstitial void locations [19].

4. Summary and conclusions

We have utilized an oblique shock loading arrangement to compact and bond small diameter solid and hollow cylinders of type 304 stainless steel and solid cylinders of tungsten. These consolidation experiments approximate 2-dimensional compaction and

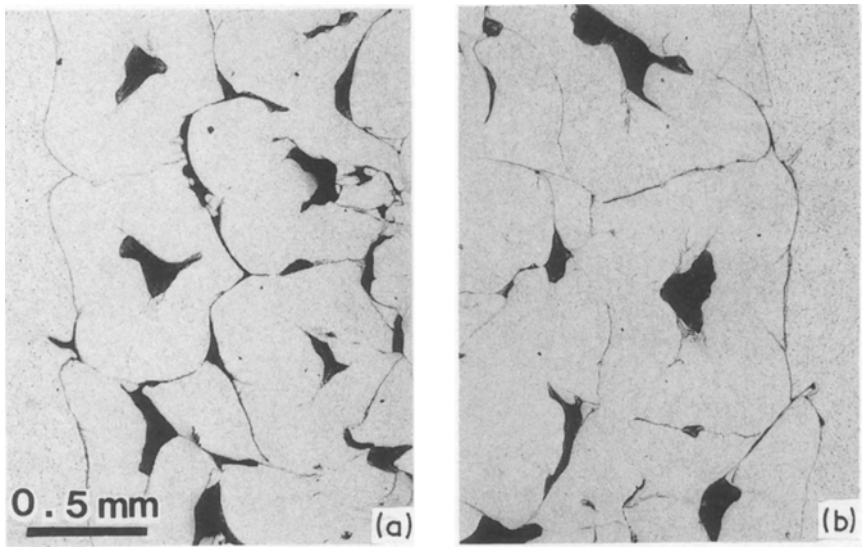

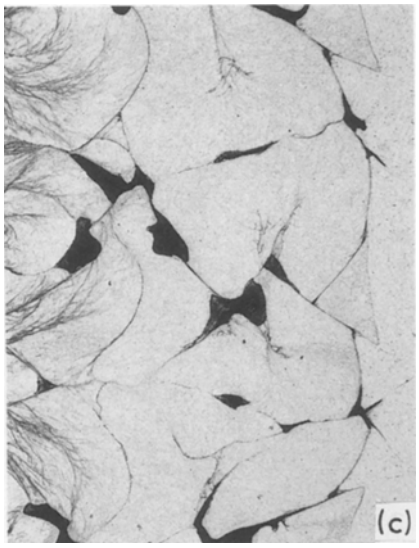

Figure 10 Metallographic section views for a series of implosively consolidated, monosize 304 stainless steel tubes. (a) 1.1 mm diameter tubes, (b) 1.5 mm diameter tubes, (c) 1.8 mm diameter tubes.

consolidation when viewed parallel to the cylindrical axes. Such 2-dimensional experiments can be accurately modelled in comparison to 3-dimensional consolidation of monosize spheres which can only be inferred from such modelling [17–19].

Melting was observed to be localized at void spaces or interstices between contacting cylinders after oblique shock loading indicating two sources of heating: void collapse and particle deformation. The void collapse is associated with localized straining to fill the void space, and the heat arises from the localized adiabatic straining at high strain rate. This straining increases for increasing void volume or interstitial volume, and local heating is, therefore, related to the cylinder diameters and size distribution, which directly influences interstitial volume. In both stainless steel and tungsten solid cylinders, the local, interstitial melting or melt fraction increased with increasing void volume or void space. Conversely, melt fraction increased with cylinder diameter. Consistent with this observation, the melt fraction was more prominent in the centers of initially hollow stainless steel cylinders than solid cylinders when the central void volume was greater than the interstitial volume (or area in the context of a 2-dimensional approximation). Consequently, it was demonstrated that melt spikes or localized melting can be controlled by manipulating the interstitial or void volume or void space in a 2-dimensional regime. Such manipulation is achieved by using a distribution of cylinder sizes, or particle sizes if extended to a 3-dimensional regime.

In addition, the melt fraction for any particular cylindrical geometry (or size distribution) increased with increasing peak pressure. This observation was accurately characterized by the 2-dimensional modelling developed by Flinn *et al.* [19] and previously applied to the 3-dimensional dynamic consolidation of 304 stainless steel powders. While in the previous model applications it was inferred that the representation applied to the 3-dimensional powder regime, the present results for cylinders are more accurately modelled 2-dimensionally, and lend further support to the inferences already made regarding the dynamic consolidation of powders.

The following specific conclusions restate the most significant aspects of this investigation:

1. Oblique shock loading of solid and hollow cylinders of 304 stainless steel and tungsten has demonstrated that melting during consolidation occurs at localized hot spots which coincide with the interstitial or other void spaces prior to compaction and consolidation.

2. The localized hot spots observed in explosively consolidated cylinders of stainless steel and tungsten are accurately modelled and predicted by 2-dimensional, microlevel numerical calculations recently developed by Flinn *et al.* [19].

3. The localized hot spots observed in this study demonstrate that assumptions of uniform energy deposition during dynamic consolidation of 3-dimensional particles (or powders) are unsubstantiated.

4. Hot spots and localized melting during consolidation of metal or alloy cylinders observed in this investigation arise by the extrusion of material to fill the interstitial or other void space and, therefore, originates by strain heating and localized deformation.

5. The larger the interstitial or other void space, the larger the strain heating at these locations, and con-

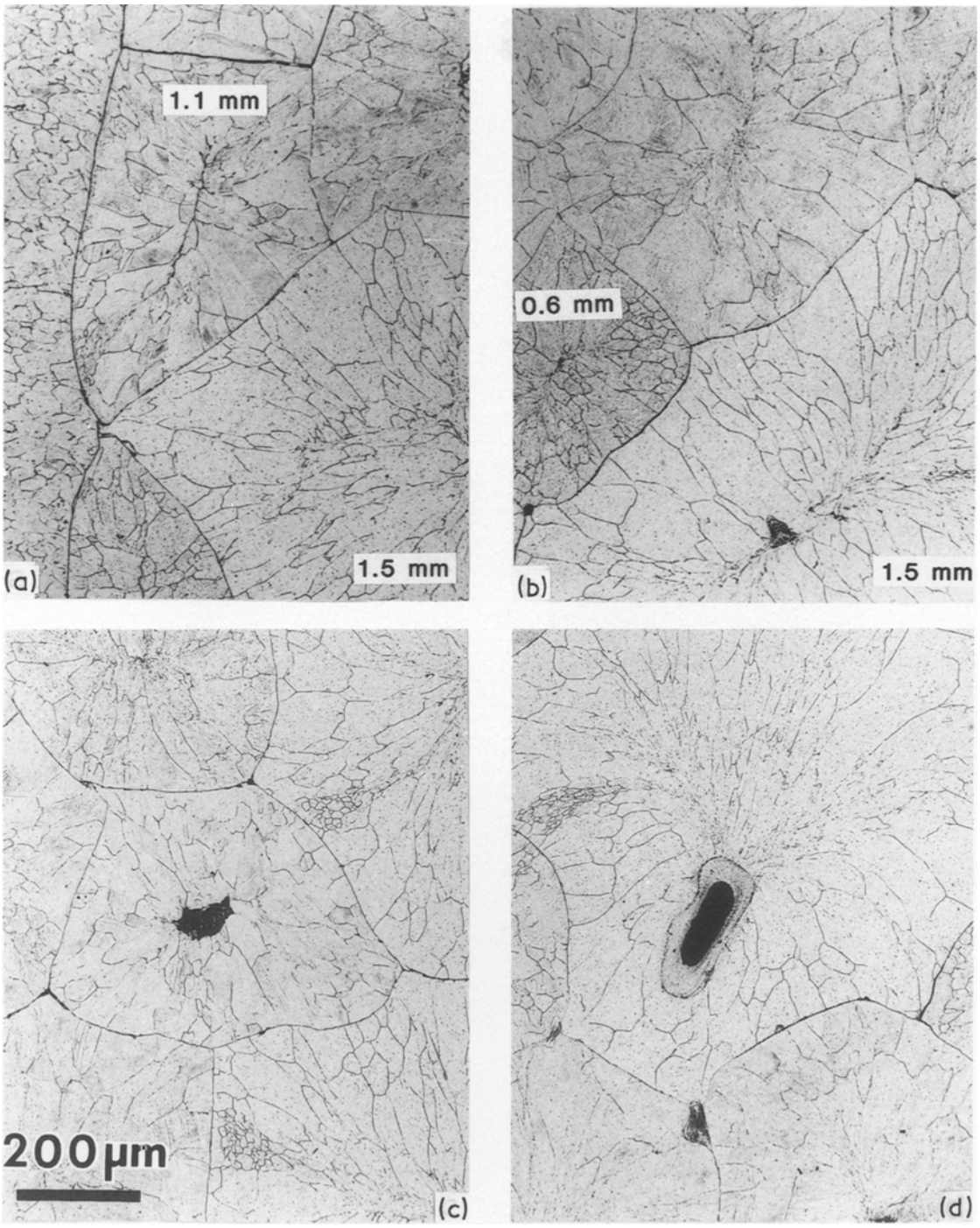

Figure 11 Enlarged metallographic cross-section views showing a series of implosively consolidated, multi-size (trimodal distribution) of 304 stainless steel tubes at different peak pressures: (a) 12 GPa, (b) 14 GPa, (c) 17 GPa, (d) 20 GPa. The three starting tube sizes were 0.6 mm, 1.1 mm, and 1.5 mm diameter, as indicated in the views shown in (a) and (b).

comitant melting. By filling larger void spaces with smaller or distributed cylinder sizes and reducing the void space, the localized heating and melting is reduced. Extrapolated to 3-dimensional powder regimes, this means that heating and melting overall during explosive (or dynamic) consolidation can be reduced (and controlled) through appropriate selection of particle size and size distributions.

6. The localized heating and melting at interstitial void sites or other void spaces within any specific cylindrical regime having a fixed distribution of sites or any particular diameter of cylinders was observed to increase with increasing peak shock pressure for a constant pulse duration (or time of pressure application).

Acknowledgement

We are grateful for comments on this manuscript by R. L. Williamson of INEL, and for the provision of model results acknowledged in Figs 7 and 8. Discussions of this work with K. A. Johnson of LANL are also gratefully acknowledged. K.P.S. is also grateful for support through an Alexander von Humboldt Senior Scientist Award for 1988–89.

References

1. V. D. LINSE in "Metallurgical Applications of Shock-Wave and High-Strain-Rate Phenomena", edited by L. E. Murr, K. P. Staudhammer, and M. A. Meyers, (Marcel Dekker, Inc., New York, 1986) pp. 29–55.
2. T. TANIGUCHI, K. KONDA and A. SAWAOKA, *ibid.*, pp. 293–311.

3. M. L. WILKINS, A. S. KUSUBOV and C. F. CLINE, *ibid.*, pp. 57–82.
4. D. G. MORRIS, *Mater. Sci. Engr.* **57** (1983) 198.
5. M. A. MEYERS, B. B. GUPTA and L. E. MURR, *J. Metals* **33** (1981) 21.
6. R. B. SCHWARTZ, P. KASIRAJ, T. VREELAND Jr and T. J. AHRENS, *Acta Metall.* **8** (1984) 1243.
7. W. H. GOURDIN in "Shock Waves in Condensed Matter", edited by J. R. Asay, R. A. Graham, and G. K. Straub (Elsevier Science, New York, 1984) p. 379.
8. W. H. GOURDIN *J. Appl. Phys.* **55** (1984) 172.
9. T. VREELAND Jr, P. KASIRAJ, A. H. MUTZ and N. N. THADHANI, in "Metallurgical Applications of Shock-Wave and High-Strain-Rate Phenomena", edited by L. E. Murr, K. P. Staudhammer, and M. A. Meyers (Marcel Dekker, Inc., New York, 1986) pp. 231–246.
10. J. E. SMUGERESKY and W. H. GOURDIN, *ibid.* pp. 107–128.
11. K. P. STAUDHAMMER and K. A. JOHNSON, *ibid.* pp. 149–166.
12. L. E. MURR, S. SHANKAR, A. W. HARE and K. P. STAUDHAMMER, *Scripta Met.* **17** (1983) 1353.
13. L. E. MURR in "Metallurgical Applications of Shock-Wave and High-Strain-Rate Phenomena", edited by L. E. Murr, K. P. Staudhammer, and M. A. Meyers (Marcel Dekker, Inc., New York, 1986) pp. 329–341.
14. C. F. CLINE and R. W. HOPPER, *Scripta Metall.* **11** (1977) 1137.
15. S. V. NAIR and J. K. TIEN, *Metall. Trans.* (*A*) **18** (1987) 97.
16. V. F. LOTRICH, T. AKASHI and A. SAWAOKA, in "Metallurgical Applications of Shock-Wave and High-Strain-Rate Phenomena", edited by L. E. Murr, K. P. Staudhammer, and M. A. Meyers (Marcel Dekker, Inc., New York, 1986) pp. 277–292.
17. R. L. WILLIAMSON and R. A. BERRY, "Microlevel Numerical Modeling of the Shock-Wave Induced Consolidation of Metal Powders", in *Shock Waves in Condensed Matter*, edited by Y. M. Gupta (Plenum, New York, 1986) p. 341.
18. R. N. WRIGHT, G. E. NORTH and J. E. FLINN, *Adv. Mater. & Processes*, **132** (1987) 56.
19. J. E. FLINN, R. L. WILLIAMSON, R. A. BERRY, R. N. WRIGHT, Y. M. GUPTA and M. WILLIAMS, *J. Appl. Phys.* **64** (3) (1988) 1446.
20. M. A. MEYERS and S. L. WANG, *Acta. Metall.* **36** (4) (1988) 925.

Received 31 January
and accepted 24 August 1989.